



HAL
open science

Eco-designed Conformable Inorganic Electronics to Improve the End of Life of Smart Objects: Sensor Processing and Applications

Maxime Harnois, Fatima Garcia-Castro, Gaëtan Herry, Olivier De Sagazan,
France Le Bihan

► To cite this version:

Maxime Harnois, Fatima Garcia-Castro, Gaëtan Herry, Olivier De Sagazan, France Le Bihan. Eco-designed Conformable Inorganic Electronics to Improve the End of Life of Smart Objects: Sensor Processing and Applications. *ACS Applied Electronic Materials*, 2020, 2 (2), pp.563-570. 10.1021/ac-saelm.9b00807 . hal-02651031

HAL Id: hal-02651031

<https://univ-rennes.hal.science/hal-02651031>

Submitted on 4 Jun 2020

HAL is a multi-disciplinary open access archive for the deposit and dissemination of scientific research documents, whether they are published or not. The documents may come from teaching and research institutions in France or abroad, or from public or private research centers.

L'archive ouverte pluridisciplinaire **HAL**, est destinée au dépôt et à la diffusion de documents scientifiques de niveau recherche, publiés ou non, émanant des établissements d'enseignement et de recherche français ou étrangers, des laboratoires publics ou privés.

1
2
3
4
5
6
7 Eco-designed conformable Inorganic Electronics to
8
9
10
11 Improve the Smart Object End of Life: sensor's
12
13
14
15 processing and applications.
16
17
18
19

20 *Maxime Harnois*, Fatima Garcia Castro, Gaëtan Herry, Olivier De Sagazan, France Le Bihan*
21
22

23
24
25
26
27 Université Rennes 1, Institut d'Électronique et des Télécommunications de Rennes,
28

29
30 UMR CNRS 6164, Département Microélectronique & Microcapteurs, Campus de
31

32
33
34 Beaulieu, 35042 Rennes Cedex, France
35
36

37
38
39 KEYWORDS: Inorganic strain sensors; Conformable Electronics; Water Soluble
40

41
42 Electronics; WEEE Standard; Ecodesigned Electronics.
43
44

45
46 ABSTRACT.
47

48 The plastic pollution is indisputable and technologies aiming to add flexible electronics onto
49 objects have to take into consideration such environmental issue. Faced with this challenge, the
50 development of technologies that comply with current standards such as WEEE (Waste Electric
51 and Electronic Equipment) legislation is crucial. Green electronics based on fully biodegradable
52
53
54
55
56
57
58
59
60

1
2
3 materials is under development but needs time to be put on the market. Meanwhile, inorganic
4 electronic remains a good candidate. Consequently, it makes sense to transfer inorganic electronics
5 onto objects before it dismantling and recoveries.
6
7

8
9
10 Here, an eco-designed technology allowing the transfer of electronics onto objects is detailed.
11 Silicon-based devices are transferred from polyimide substrate (PI) to water-soluble substrate
12 (PVA: Poly(vinyl alcohol)). It is highlighted that the transfer of inorganic layers from PI to PVA
13 substrate does not have a negative impact on the devices mechanical and electrical characteristics.
14
15 To demonstrate such concept, strain gauges and temperature sensors have been transferred onto
16 daily life object reaching the same performances than sensors fabricated onto polyimide substrate.
17
18 Moreover, materials transferred onto the object using PVA substrate can be dismantled and
19 recovered at the end of object's life highlighting that hydrosoluble substrate is a good candidate
20 towards an eco-designed technology.
21
22
23
24
25
26
27
28
29
30
31
32
33

34 **1. Introduction**

35
36 High-tech products are becoming essential in our daily life promoting a constant growth
37 of the electronic industry. Thus, the everyday objects are smarter and smarter as
38 embedded electronics giving them extra functionalities.¹ However, our new consumption
39 needs must not be done, once again, at the expense of the environment. Faced with this
40 challenge, Extended Producer Responsibility (EPR) principle has been established by the
41
42
43
44
45
46
47
48
49
50
51
52
53
54 Organization for Economic Cooperation and Development (OECD).² This is a cornerstone
55
56
57
58
59
60

1
2
3 principle of waste prevention and reduction policy. The basic idea of EPR is to hold
4
5
6
7 producers responsible for the environmental impact of their products at the end of life
8
9
10 pushing them to change their practices towards the eco-design (also called design for
11
12 environment activities) and the respect of the Waste Electric and Electronic Equipment
13
14 (WEEE) legislation (Directive 2002/96/EC of the European Parliament and of the
15
16
17 Council).^{3,4} Consequently, eco-designed fabrication processes taking into consideration
18
19
20
21 the smart object end of life should be developed to respect the WEEE legislation. Up to
22
23
24 know, this aspect is overlooked in works dealing with novel technologies development
25
26
27 especially in the field of new generation of electronics such as “plastic electronics”.

28
29
30
31
32
33
34
35 In the near future, connected objects will embed sensors,^{5,6} displays,^{7,8} photovoltaic
36
37
38 panels,^{9,10} antennas,^{11,12} etc. not only into but also at the surface of the object. Among
39
40
41 technologies developed to intimately wrap electronics onto 3D objects, those using
42
43
44
45 polymeric substrates (flexible or even stretchable) are frequently reported. This last 15
46
47
48 years, research has focused on materials and methods to improve devices performances
49
50
51 and conformability instead of environmental concerns or even circular economy. Indeed,
52
53
54
55
56
57
58
59
60

1
2
3 original concepts have been developed such as ultrathin electronics,^{9,13} stretchable
4
5
6
7 electronics^{14–17} or even thermoforming technologies.¹⁸ However, polymeric substrates
8
9
10 (e.g., polyimide: PI, Polyethylene terephthalate: PET, Polyethylene naphthalate: PEN,
11
12
13 parylene, polydimethylsiloxane: PDMS ...) are permanently stuck onto the 3D object that
14
15
16
17 negatively impact Electric and Electronic Equipment (EEE) recycling.
18
19

20
21 Recently, a number of biodegradable polymers, e.g. cellulose, chitin, silk, etc. have been
22
23
24
25 considered as substrates for environmental concerns or even for the fabrication of
26
27
28 implantable electronics, piezoelectric energy harvester.^{19–23} Biodegradable substrates
29
30
31
32 can lead to the same results in term of conformability than classical polymeric substrate
33
34
35
36 however they are not compatible with clean room processing (e.g., the photolithography
37
38
39 or the wet etching steps). To overcome this challenge, novel fabrication methodologies
40
41
42
43 have to be developed.²⁴
44
45

46
47 Here, a comparative study between inorganic strain sensors fabricated onto polyimide substrate
48
49 and water soluble substrate is detailed. It will be shown that the process developed to transfer the
50
51 inorganic layer from PI to PVA substrate Poly(vinyl alcohol) did not have a negative impact on
52
53
54 the devices electrical characteristics. Note that, the process described in this work cannot be
55
56 considered as eco-friendly because it meets all the perquisites of standard cleanroom
57
58
59
60

1
2
3 manufacturing (chemical etching, photolithography, etc.) and can be transferred to the industry
4
5 (contrary to green electronics, to date). However, the concept describes in the last section can be
6
7 considered as eco-designed because it will highlights that hydrosoluble substrate is a good
8
9 candidate facing smart object recycling issues because inorganic devices can be unmounted from
10
11 the object surface to be recovered.
12
13
14
15
16

17 **2. Results and Discussion**

21 **a. Inorganic processing onto hydro-soluble substrate**

22
23
24 The figure 1 highlights the fabrication process of multilayered devices transferred onto a PVA
25
26 substrate. The process is fully compatible with cleanroom fabrication even if the targeted substrate
27
28 is water soluble. Experimental parameters are fully detailed in the experimental section. As shown
29
30 in figure 1a, at first, a PDMS layer was spin coated on a silicon carrier substrate and cured. A
31
32 25 μ m thick polyimide (PI) substrate was laminated onto the PDMS (figure 1b). The adhesion
33
34 forces between PDMS and PI are strong enough to provide a good sticking during the whole
35
36 process. The 3D scheme in the figure 1c shows that multilayered thin films can be deposited and
37
38 patterned at lithographical accuracy. Here, resistors made of two inorganic layers were fabricated.
39
40 Electrodes and resistive layers were made of aluminum and silicon, respectively. As shown in the
41
42 figure 1d, the PVA solution was spin coated following the protocol already described in a previous
43
44 work.¹⁷ As a results, the inorganic devices were sandwiched between the PI and the PVA layers
45
46 (figure 1e). The total thickness of the structure was approximately equaled 55 μ m and was flexible.
47
48 The multilayered flexible substrate can be easily peeled off from the PDMS and flipped on it.
49
50
51
52
53
54 Thus, the PVA substrate adheres to the PDMS. Indeed, PDMS is well known to adheres to many
55
56
57
58
59
60

1
2
3 kind of surfaces as it is extensively used in microfluidics for instance.²⁵ Note that, the PDMS
4 substrate can be reused from one process to another. The last stage consists in the dry etching of
5 the PI films using O₂ plasma. After PI films fully-etching, the inorganic devices was transferred to
6 the PVA substrate as shown in the 3D schemes of figure 1g and in the optical pictures of the figures
7 1h and 1i.

8
9
10
11
12
13
14 The figure 1k highlights the time sequence of the PVA substrate dissolution. Note that, in the
15 figure 1h, a PI ring remains after dry etching of the PI substrate. This etching residue is due to the
16 mechanical clamp used to fix the wafer during the etching stage. The top left image of the figure
17 1k highlights that a part of the flexible substrate is composed of a PVA film (transparent area) as
18 substrate and a sandwich of PVA and PI (i.e., the dark yellow etching residue). In the figure 1k,
19 after approximately 90 seconds, The PVA substrate was fully dissolved in water whereas the PI
20 substrate was intact with inorganic material remaining on it. Consequently, the fabrication process
21 does not damaged the PVA substrate and especially it ability to be dissolved in water.
22
23
24
25
26
27
28
29
30
31
32
33
34
35
36
37
38
39
40
41
42
43
44
45
46
47
48
49
50
51
52
53
54
55
56
57
58
59
60

b. Inorganic strain sensor

Inorganic strain sensors were fabricated on two kinds of substrates: a 25 μ m thick
Polyimide and a 30 μ m thick PVA substrate. As shown in Figure 2, their response to
mechanical strain were analyzed in static (as function of bending radius) and dynamic

1
2
3 modes (voltage and resistivity as function of time and applied strain). In static mode
4
5
6
7 (figures 2a, 2b and 2c), the protocol consists in the measurement of the current as
8
9
10 function of the voltage in the range of plus to minus 1V when substrate is flat (bending
11
12
13 radius equals 0). It allows to determine the initial value of the resistivity. Then, the
14
15
16 substrates were fixed to a tensile bending tools (half cylinders) and were bent from the
17
18
19 lowest curvature (i.e., the lower applied strain) to the highest curvature (i.e., the highest
20
21
22 applied strain). The bending radii were fixed to 0 (flat), 2.5 (R1), 2 (R2), 1.5 (R3) and 1
23
24
25
26
27
28 cm (R4).
29
30
31

32 Then, the gauge factor (GF) is used to qualify the sensitivity of strain sensors fabricated
33
34
35 onto the PVA and the PI substrate as shown in figures 2b and 2c, respectively. GF is
36
37
38 defined by the Equation (1) as the ratio of the relative change of the sensors resistivity
39
40
41
42
43 ($\Delta R/R_0$) and the strain ϵ applied to the sensor:
44
45
46

$$GF = \frac{\Delta R}{R_0} \epsilon \quad (1)$$

47
48
49
50
51 For metals, GF is low, between 2 and 5²⁶ whereas for semiconductors such as silicon,
52
53
54
55 GF exhibits much larger values around 100 for single crystalline silicon (sc-Si), between
56
57
58
59
60

1
2
3 20 and 40 for poly crystalline silicon (poly-Si) ²⁷ or 20–30 for amorphous silicon (a-Si) ²⁸.
4
5

6
7 In this work, microcrystalline silicon is deposited. The SG has already been determined
8
9
10 in previous works and is fixed to 80GPa ²⁹. Here, the strain (ϵ) applied to the structure is
11
12
13 function of the radius of curvature. ϵ is calculated using the already proposed model for a
14
15
16
17 bi-layer device taking into consideration their thicknesses and their Young modulus (Y).²⁹
18
19

20
21
22 In this work, the material properties and device structure are presented in the figure 1 and
23
24
25 the Table S1 of the supporting information. This model takes into account the substrate
26
27
28 and the stiffest layer (i.e. the silicon), which mainly define the mechanical behavior of the
29
30
31 device. Consequently, the bilayer model is thus constituted by the PI substrate and the
32
33
34
35 Si layer and the longitudinal strain $\epsilon_{surface}$ applied on the surface of the layer is given by
36
37
38
39 the equation (2) derived from [25]:
40
41
42
43
44
45
46

$$\epsilon_{surface} = \left(\frac{1}{r} \pm \frac{1}{r_0} \right) \left(\frac{d_s + d_f}{2} \right) \left(\frac{1 + 2\chi\eta + \chi\eta^2}{(1 + \eta)(1 + \chi\eta)} \right) \quad (2)$$

47
48
49
50
51
52
53
54
55
56
57
58
59
60

1
2
3 where r and r_0 are the applied and initial radii of curvature, respectively, d_s and d_f are
4
5
6
7 substrate and layer thicknesses, respectively, and are defined by $\chi=Y_f/Y_s$ and $\eta=d_f/d_s$,
8
9
10 where Y_s and Y_f are substrate and layer Young moduli, respectively. The plus (or minus)
11
12
13 signs depends on applied bending opposite to (or with) the built-in curvature. The silicon,
14
15
16
17 the PI and the PVA thicknesses were measured and were equaled 100nm, 25 μ m and
18
19
20
21 30 μ m, respectively. To calculate the strain, the young modulus of the PI and the PVA
22
23
24 substrates have been fixed to 5GPa³⁰ and 1.9GPa, respectively, according to the
25
26
27
28 literature.¹⁶
29
30
31

32
33 Figures 2b and 2c show that SG values equal -21 and -24 for sensors fabricated onto
34
35
36 PVA and PI, respectively. It can be notice that the collected data points (see in figure 2b)
37
38
39 corresponding to the highest strain value has not been taken into consideration in the
40
41
42 calculation of GF. Indeed, as shown in figure S1, when the strain exceeds approximately
43
44
45
46 0.14% cracks occur in the silicon layer leading to drastically increases the strain sensors
47
48
49 resistivity. An option to decrease the strain is to reduce the substrate thickness (d_s).
50
51
52
53 Indeed, as shown in figures 2b and 2d, at same radius of curvature, the applied strain in
54
55
56
57
58
59
60

1
2
3
4 PI is lower than the applied strain in PVA mainly because the PVA substrate was 5 μ m
5
6
7 thicker than the PI substrates. However, it is demonstrated that the sensitivity and the
8
9
10 mechanical behavior of the strain sensors is in the same order of magnitude proving that
11
12
13 the fabrication process does not impact the strain sensors response.
14
15
16
17

18 As shown in the figures 2d, 2e and 2f, the strain sensors have been mounted onto a
19
20
21 rubber based membrane submitted to a differential pressure (see also in the
22
23
24 supplementary figure S2). Each 5 seconds, a pulse of 900 mbar is applied onto the
25
26
27 membrane that deforms the sensors (Elveflow pressure controller; MK3). The value of
28
29
30 the sensor resistivity is recorded, amplified and converted in voltage using analogic
31
32
33 circuits in combination with Arduino Uno development Kit.
34
35
36
37
38
39

40 The variation of the voltage as function of time is plotted in the figures 2e and 2f. It
41
42
43 highlights that whatever the substrate a signal can be recorded showing a good response
44
45
46 of the sensors in dynamic mode. Finally, sensors have been mounted onto the finger joint
47
48
49 of a nitrile glove. The variation of the resistivity as function of the finger motion is recorded
50
51
52
53 and shown in the figures 2g, 2h and 2i. These experiments highlight that inorganic strain
54
55
56
57
58
59
60

1
2
3 gauge fabricated onto PVA substrate can be used as sensors for prosthetic hands has
4
5
6
7 already demonstrated for these fabricated onto other plastic substrates.³¹⁻³³ However, the
8
9
10 main difference can rely on the WEEE management of such devices has demonstrated
11
12
13
14 in the next section.

18 **c. WEEE management**

19
20 On the one hand, significant challenges in the management of WEEE are the dismantling
21
22
23 and the recovery of materials.³⁴ On the other hand, it can be anticipated that most of our
24
25
26
27 future products will embed electronics. For instance, daily life objects such as a T-Shirt
28
29
30 that will embed sensors or RFID Tag will be not considered as a T-shirt from recycling
31
32
33
34 point of view, but as a WEEE. Consequently, the objects' end of life must be taken into
35
36
37
38 consideration when a new technology is developed in order to respect the eco-design
39
40
41
42 rules already fixed by the legislation. It is the case of flexible electronics, the results
43
44
45 detailed in the previous section and in the literature have demonstrated that plastic
46
47
48 electronics can conformably wrap daily life object. However, the question of the EoL is
49
50
51
52 not taken into consideration. For instance, when plastic foils will be stuck onto the object,
53
54
55
56 can the electronics devices be separated easily from the object? Furthermore, when
57
58
59
60

1
2
3 devices are fabricated onto conventional plastics such as PI substrates, is device's
4
5
6 materials can be dismantled from the substrate? From recovery point of view, some of
7
8
9 most interesting materials are metals. Is it possible to recovery the pure metals and reuse
10
11
12 them as high grade electronics materials? In future works, these questions cannot be
13
14
15 avoid and need to be systematically taken into consideration.
16
17
18
19

20
21 This section highlights that the technology based on water soluble substrate to transfer
22
23 inorganic devices onto daily life objects fits the requirement of the WEEE legislation as
24
25 materials can be recovered. Moreover, the daily life object can be reused. To take benefit
26
27
28 from PVA as sacrificial layer from WEEE recycling point of view, resistive inorganic
29
30
31 temperature sensors have been conformably wrapped onto a daily life object (a cup). The
32
33
34 following experiments illustrate our concept and highlight how inorganic material can be
35
36
37 recovered after the object lifecycle.
38
39
40
41
42
43
44

45
46 The figures 3a, 3b and 3c show the daily life object (a cup), inorganic resistors fabricated
47
48
49 onto PVA substrate and the devices transferred onto an edge of the cup, respectively.
50
51
52

53
54 Different technologies based on the concept of water assisted transfer can be used to
55
56
57
58
59
60

1
2
3 provide a conformal wrapping of devices onto an object. All benefit from water to partially
4
5
6
7 or fully dissolve the hydrosoluble substrate to transfer the devices. They are named tattoo
8
9
10 electronics,³⁵⁻³⁷ water transfer printing,^{6,38,39} hydroprinting, etc.⁴⁰ Furthermore, previous
11
12
13 works have demonstrated that the water transfer printing is a convenient technology to
14
15
16
17 fabricate large area electronics answering industrial issues.⁴¹
18
19
20
21

22 In this work, the external part of the cup has been humidify and the PVA substrate has
23
24
25 been stuck to the external wall of the cup. Consequently, has already shown by Rogers
26
27
28 et al. the bottom face of the PVA substrate is partially dissolved and conformably adheres
29
30
31 to the object.⁴² The figure 3d highlights that the resistive temperature sensor is still
32
33
34
35 working after it conformal mounting on the cup. One can notice that the value of the
36
37
38 resistance equals 47.2 KOhm that is in the same range than for the experiments in the
39
40
41 figure 2. This step can be considered as the testing step of a smart daily life object.
42
43
44
45

46 The figure 3e shows the evolution of the temperature inside (black curve) and in the external part
47
48 of the cup wall (red curve) when the cup is filled with boiling water and cool down. The
49
50 temperature inside and outside the wall has been measured using a k-probe thermocouple and an
51
52 IR-thermometer, respectively. As expected, the two temperatures follow the same trend, and the
53
54 temperature on the external part of the wall is systematically lower than the temperature inside.
55
56
57
58
59
60

1
2
3 Furthermore, when the cup is filled with boiling water, the temperature inside the cup grows up
4 faster than this on the external part of the wall cup as also expected. The blue curve shows the
5 variation of the sensor resistivity as function of the temperature. The trend of the blue curve follows
6 the same behavior than the temperature measured using the IR-thermometer showing that the
7 temperature at the surface of a daily life object can be monitored. The figure 3f highlights the
8 dissolution of PVA when the cup is dipped into the water. It highlights the dismantling of the
9 inorganic layer from the object. Indeed, as shown in the figure 3f, the PVA is fully dissolved after
10 150 seconds detaching the inorganic devices. Thus, the object and the inorganic materials (after
11 water filtration) can be recovered to be reused as shown in the figures 3g and 3h, respectively. At
12 this step, two alternative can be chosen: object and inorganic materials can be recycled (second
13 life) or destroyed following the WEEE standards. In both cases, this smart object end of life will
14 be improved thanks to the eco-designed technology developed in this work. Moreover, even if
15 silicon based materials remains in water, such inorganic nanomembrane will be fully dissolved as
16 already reported in literature.^{43,44}

35 **3. Conclusion**

36 Due to harmful aspects of human activity, our Mother Earth is facing environmental concerns.
37 Plastic pollution is one of these environmental issues and the new generation of electronics that
38 will flexible, stretchable, etc. have to take into consideration these issues. Here, a technologies
39 allowing to wrap inorganic devices onto 3D object is reported. In addition to save electrical and
40 mechanical capabilities, devices performed onto water soluble substrate can be dismantled from
41 the object and recovered. Furthermore, it can be anticipated that other eco-friendly materials that
42 can be put into solution can be compatible with the process described in this works.

4. Experimental Section

a. Characterization:

Top-view images were obtained by PENTAX K70D equipped with a ZOOM macro 50mm (Pentax). Static I(V) electrical characteristics of the devices were collected at room temperature using an Agilent B1500A semiconductor parameter analyzer. Temperature were measured using a Fluke 51 II thermometer using an K-probe (Ohmega) and a Fluke 62 Max IR-thermometer.

b. Fabrication

PDMS adhesion layer: Sylgard 184 PDMS was purchased from Dow Corning (Midland, U.S.A.), mixed with curing agent at a mass ratio of 10:1, and degassed for 30 min before spin-coating. Spin-coating parameters (velocity = 300 rpm; acceleration = 50 rpm.s⁻¹; duration = 60 s) were kept constant for all the experiments (i.e., after curing, such spin-coating parameters allow the fabrication of 300µm thick PDMS on silicon substrates).

1
2
3
4 Polyimide Substrate: A 25 μm thick substrate of PI (DuPontTM France) were manually
5
6
7 laminated onto the PDMS. Air bubbles trapped between PI and PDMS were removed
8
9
10 under vacuum.

11
12
13
14
15 *PVA processing:* a PVA solution (PVA; Mw 9000-10000, 80% hydrolyzed from Aldrich)
16
17
18 was prepared by mixing DI (deionized) water and PVA powder (5:1 w/w water/PVA) and
19
20
21 filtering it with a 0.4 μm filter. The PVA is filtered to avoid any aggregates. This step allows
22
23
24 the fabrication of a PVA surfaces as smooth as possible (nanometric scale).PVA was
25
26
27 spin-coated on PI substrates to form a 30- μm -thick layer and baked at 100°C for 2 hours.
28
29
30
31
32 The spin-coating was performed at low rotation velocity 20 rpm and acceleration 10 rpm
33
34
35 s⁻¹ for uniform thickness.

36
37
38
39
40 *Inorganic Thin film patterning:* A 150-nm-thick aluminum film was deposited by thermal
41
42
43 evaporation at a deposition rate of 0.2 nm s⁻¹. A classical lithographic process using
44
45
46 S1818 (Dow electronic material MICROPOSIT) as photoresist (velocity = 4500 rpm;
47
48
49 acceleration =5000 rpm s⁻¹; duration = 60 s) was performed to pattern the aluminum
50
51
52
53
54 electrodes that can be both wet etched (H₃PO₄) or dry etched in ICP/RIE (inductive
55
56
57
58
59
60

1
2
3
4 coupled plasma / reactive ion etching) equipment from Corial (France) with the
5
6
7 experimental settings of 5 mTorr working pressure, 100 W plasma power, and chlorinated
8
9
10 gas flow of 30 sccm.

11
12
13
14 A 150-nm-thick silicon film was deposited by PECVD (Plasma Enhanced Chemical Vapor
15
16
17 Deposition. Experimental settings were adjusted as follows: The gazes' flow rate are fixed
18
19
20 to 1.5sccm of SiH₄, 75sccm of H₂ and 75sccm of Ar (1% dilution of SiH₄ in Ar-H₂
21
22
23 mixture), 10Sccm of AsH₃. The working pressure, the power and the temperature equals
24
25
26 0.9mbar, 15W and 165°C, respectively. 1.8 μm thick of S1818 was spin-coated (velocity
27
28
29 = 4500 rpm; acceleration =5000 rpm s⁻¹; duration = 60s) and used as mask to define
30
31
32 the active area of the resistors. The n-doped Silicon was etched using SF₆ plasma (Roth
33
34
35 and Roh equipment). The experimental parameters were adjusted as follows: The gaze
36
37
38 flow rate is fixed to 50sccm of SiH₄. The working pressure, the power and the temperature
39
40
41 equals 30mTorr, 50W and 20°C, respectively.
42
43
44
45
46
47
48
49

50 *PI substrate etching:* dry etched in ICP/RIE (Corial, France) with the experimental settings
51
52
53 of 20 mTorr working pressure, 950 W and 50W for the ICP plasma and the RF power
54
55
56
57
58
59
60

1
2
3 respectively, an oxygen and Argon gases flow of 30 sccm 50 sccm respectively was used
4
5
6
7 to etch the PI film.
8
9
10
11
12
13
14

15 **Acknowledgments**

16
17 This work is supported by the European Union through the European Regional
18
19 Development Fund (ERDF), by the French region of Brittany (project: IMPRIM'), and by
20
21
22 IETR (project: 3DELEC).
23
24
25
26
27
28
29
30
31
32
33
34
35
36
37
38
39
40
41
42
43
44
45
46
47
48
49
50
51
52
53
54
55
56
57
58
59
60

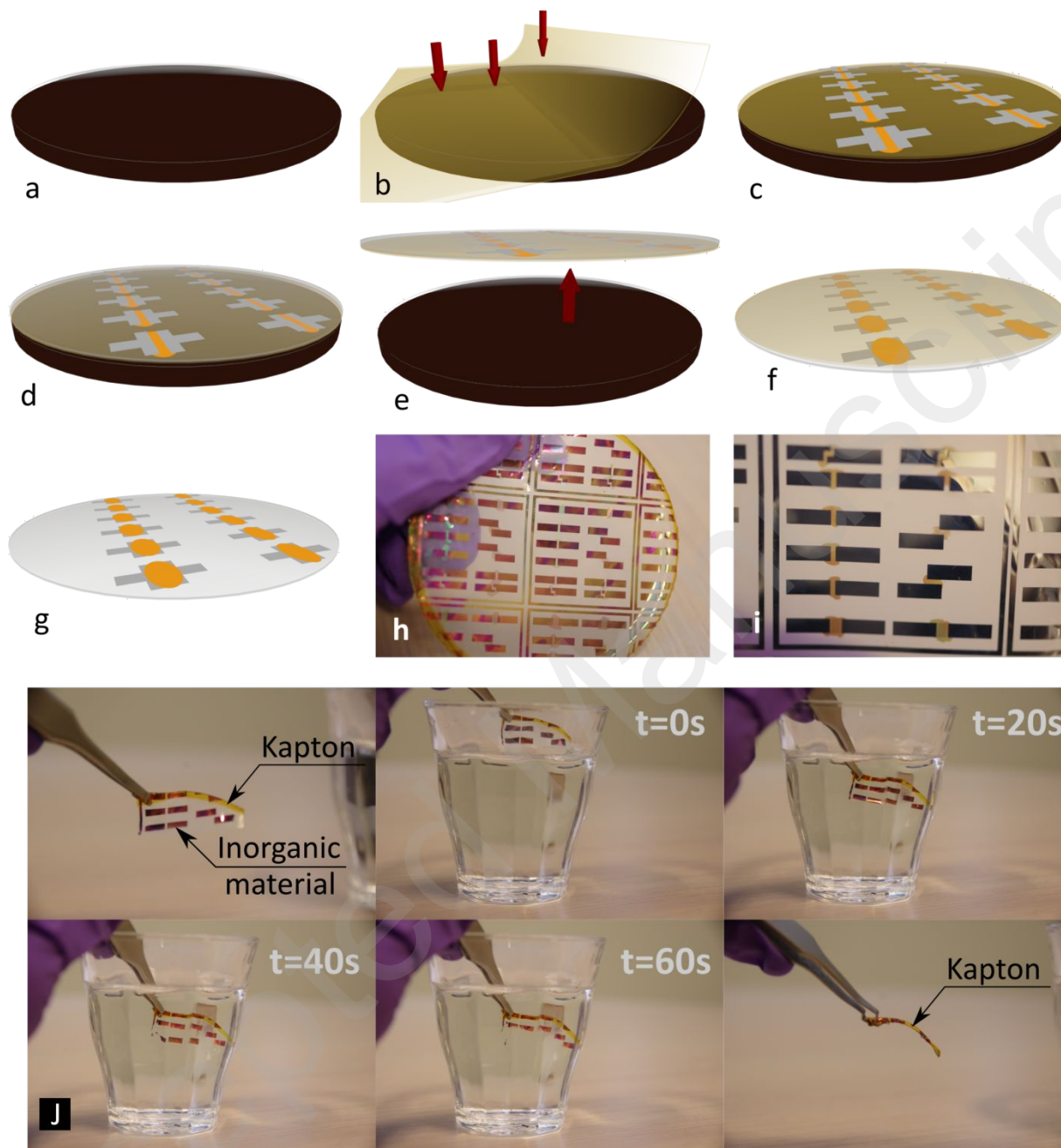
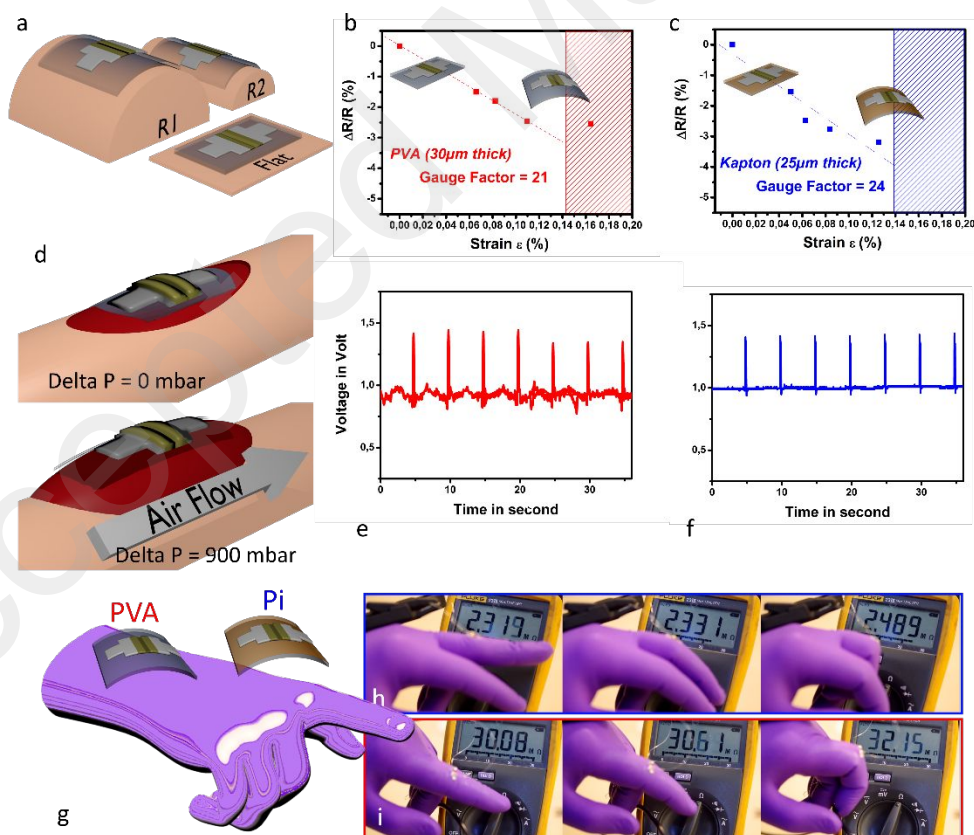


Figure 1. Inorganics multilayered electronics transferred onto PVA substrates. a) PDMS spincoated onto silicon substrate, b) PI substrate laminated onto PDMS, c) multilayered inorganic thin films patterned onto PI, d) PVA spin coating, e) PI substrates peeling from

1
2
3 the PDMS adhesive layer, f) Multilayered inorganic devices sandwiched between the PI
4 and the PVA films, g) Inorganics devices transferred to the PVA substrates after dry
5 etching of the PI substrate, h) optical picture after the PI etching; i) zoom in the devices;
6
7 and the PVA films, g) Inorganics devices transferred to the PVA substrates after dry
8 etching of the PI substrate, h) optical picture after the PI etching; i) zoom in the devices;
9
10
11
12
13
14 j) Dissolution of the PVA substrate as function of time; To evaluate quantitatively the
15 dissolution rate of PVA as function of additional external physical parameters such as
16
17
18
19
20
21
22
23
24
25
26
27
28
29
30
31
32
33
34
35
36
37
38
39
40
41
42
43
44
45
46
47
48
49
50
51
52
53
54
55
56
57
58
59
60



1
2
3
4
5
6 **Figure 2: Mechanical behavior of inorganic strain sensor fabricated onto PVA and**
7
8
9 **Polyimide.** a) 3D view of the measurement protocol in static operating mode. For both
10 technologies (PVA and Pi), the current versus the voltage is measured varying the radius
11 of curvature (flat, 5cm, 2cm, 1.5cm and 1cm); The variation of the resistivity as function
12 of applied strain for strain sensors fabricated onto: b) PI substrate and c) PVA substrate.
13
14
15
16
17
18
19
20
21
22
23 d) 3D view of the measurement protocol in dynamic operating mode; The strain sensors
24 is mounted onto a rubber membrane deformed by a differential of pressure (900mbar);
25
26
27 For both technologies (PVA and Pi) response of voltage versus time at two different
28 differential pressures (0 and 900mbar) for strain sensors fabricated onto : e) PI substrate
29
30
31 and f) PVA substrate. g) 3D view of strain sensors (PVA and PI substrates) mounted onto
32
33
34
35
36
37
38 a nitrile glove. Resistivity response varying the finger bending angle for sensors fabricated
39
40
41
42
43
44
45 onto: h) the PVA substrate and i) the PI substrate.
46
47
48
49
50
51
52
53
54
55
56
57
58
59
60

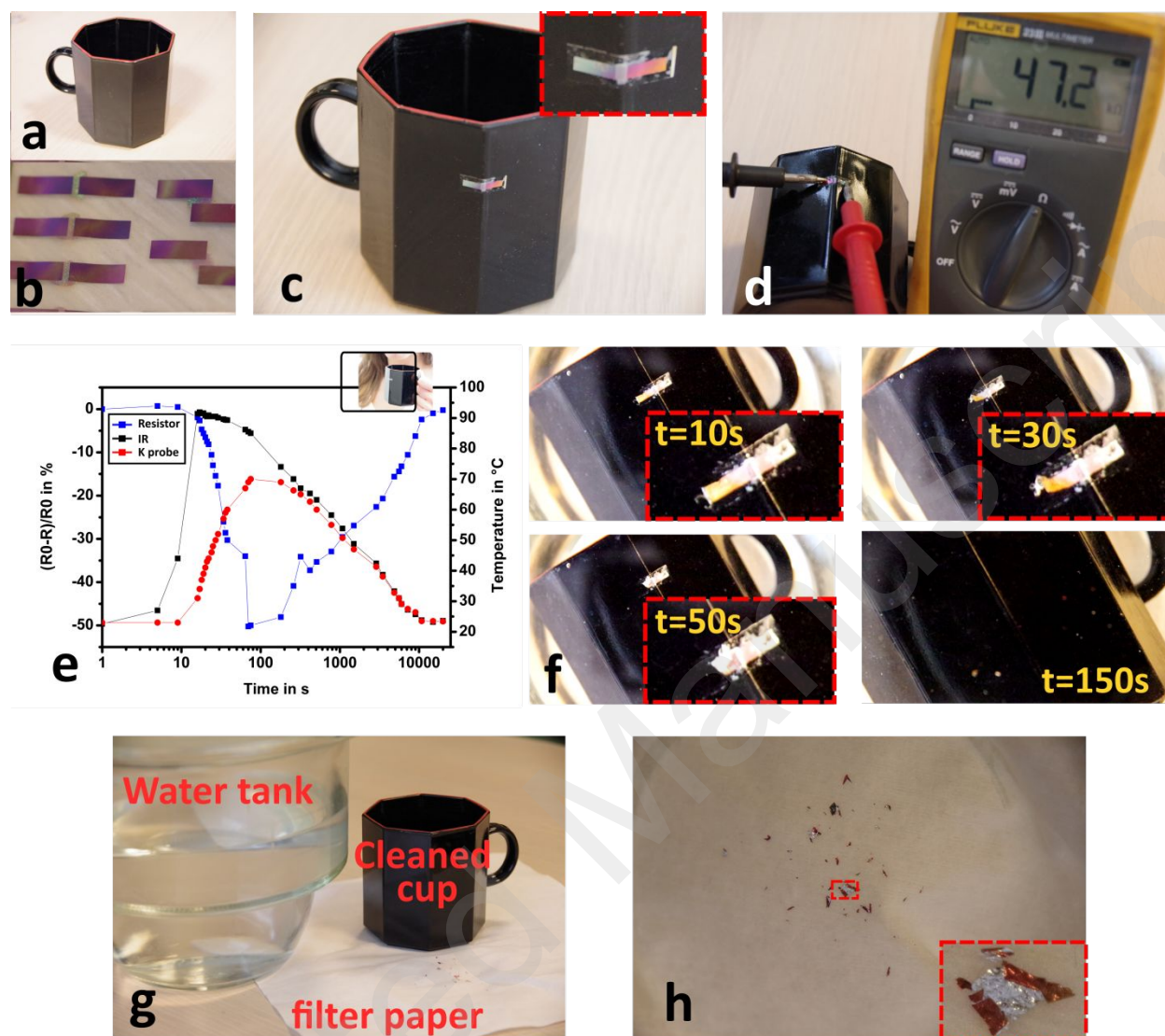


Figure 3: Ecodesigned inorganic sensor fabricated onto PVA: dissolution, transfer, dismantling and recovery. a) a cup as daily life object; b) resistor as temperature sensors fabricated onto PVA; c) water assisted transfer of the temperature sensors onto the cup. The inset highlights the inorganic device wraps onto a edge of the cup (angle =155°); d) electrical test of the resistor; e) Evolution of: i) the sensor resistivity as function of the cup

1
2
3 temperature (blue curves, left axe), ii) k-probe thermocouple (red curve, right axe), iii) IR
4
5
6
7 thermometer (black curve, right axe); f) dismantling of the inorganic device from the cup:
8
9
10 g) The cup after dismantling the inorganic devices; h) inorganic films after filtration. The
11
12
13
14 inset highlights metal and silicon.
15
16
17
18
19
20
21
22
23
24
25
26
27
28
29
30
31
32
33
34
35
36
37
38
39
40
41
42
43
44
45
46
47
48
49
50
51
52
53
54
55
56
57
58
59
60

1
2
3
4
5
6
7
8
9
10
11
12
13
14 ASSOCIATED CONTENT:
15

16
17 **Supporting information:**
18

19
20
21 Table S1: Mechanical characteristics of inorganic material that constitute the strain
22
23
24 sensor
25

26
27
28 Figure S1: Optical picture of cracks in silicon thin films due to an excess of strain.
29

30
31 Figure S2: Setup used to deform and acquire the strain sensor electrical signal.
32
33

34
35
36
37
38 AUTHOR INFORMATION
39

40
41
42 **Corresponding Author**
43

44
45
46 Dr. M. Harnois,
47
48
49
50
51
52
53
54
55
56
57
58
59
60

1
2
3
4 Université Rennes 1, Institut d'Électronique et des Télécommunications de Rennes,
5
6
7 UMR CNRS 6164, Département Microélectronique & Microcapteurs, Campus de
8
9
10 Beaulieu, 35042 Rennes Cedex, France.

11
12
13
14
15 E-mail : maxime.harnois@univ-rennes1.fr
16
17
18
19
20
21
22
23

24 **Author Contributions**

25
26
27 The manuscript was written through contributions of all authors. All authors have given
28
29
30 approval to the final version of the manuscript.
31
32
33
34

35 **ACKNOWLEDGMENT**

36
37
38
39 This work is supported by the European Union through the European Regional
40
41
42 Development Fund (ERDF), by the French region of Brittany (project: IMPRIM'), and by
43
44
45 IETR (project: 3DELEC).
46
47
48
49
50
51
52
53
54
55
56
57
58
59
60

References

- (1) Bohn, J.; Coroamă, V.; Langheinrich, M.; Mattern, F.; Rohs, M. Living in a World of Smart Everyday Objects—Social, Economic, and Ethical Implications. *Hum. Ecol. Risk Assess.* **2004**, *10* (5), 763–785.
- (2) Kibert, N. C. Extended Producer Responsibility: A Tool for Achieving Sustainable Development. *J. Land Use Environ. Law* **2004**, *19* (2), 503–523.
- (3) Goodship, V.; Stevels, A. *Waste Electrical and Electronic Equipment (WEEE) Handbook*; Elsevier, 2012.
- (4) Ongondo, F. O.; Williams, I. D.; Cherrett, T. J. How Are WEEE Doing? A Global Review of the Management of Electrical and Electronic Wastes. *Waste Manag.* **2011**, *31* (4), 714–730.
- (5) Khosla, A.; Ahmed, K.; Shiblee, M. N. I.; Thundat, T.; Nagahara, L. A.; Furukawa, H. Shape Conformable Flexible Sensors for Internet of Things (IoT): A Perspective. In *Meeting Abstracts*; The Electrochemical Society, 2018; pp 284–284.
- (6) Le Borgne, B.; De Sagazan, O.; Crand, S.; Jacques, E.; Harnois, M. Conformal Electronics Wrapped Around Daily Life Objects Using an Original Method: Water Transfer Printing. *ACS Appl. Mater. Interfaces* **2017**, *9* (35), 29424–29429.
- (7) Zhang, Z.; Cui, L.; Shi, X.; Tian, X.; Wang, D.; Gu, C.; Chen, E.; Cheng, X.; Xu, Y.; Hu, Y.; J. Zhang; L. Zhou; H.H. Fong; P. Ma; G. Jiang; X. Sun; B. Zhang; H. Peng; Textile Display for Electronic and Brain-Interfaced Communications. *Adv. Mater.* **2018**, *30* (18), 1800323.
- (8) Sekitani, T.; Nakajima, H.; Maeda, H.; Fukushima, T.; Aida, T.; Hata, K.; Someya, T. Stretchable Active-Matrix Organic Light-Emitting Diode Display Using Printable Elastic Conductors. *Nat. Mater.* **2009**, *8* (6),
- (9) Kaltenbrunner, M.; White, M. S.; Głowacki, E. D.; Sekitani, T.; Someya, T.; Sariciftci, N. S.; Bauer, S. Ultrathin and Lightweight Organic Solar Cells with High Flexibility. *Nat. Commun.* **2012**, *3*, 770.

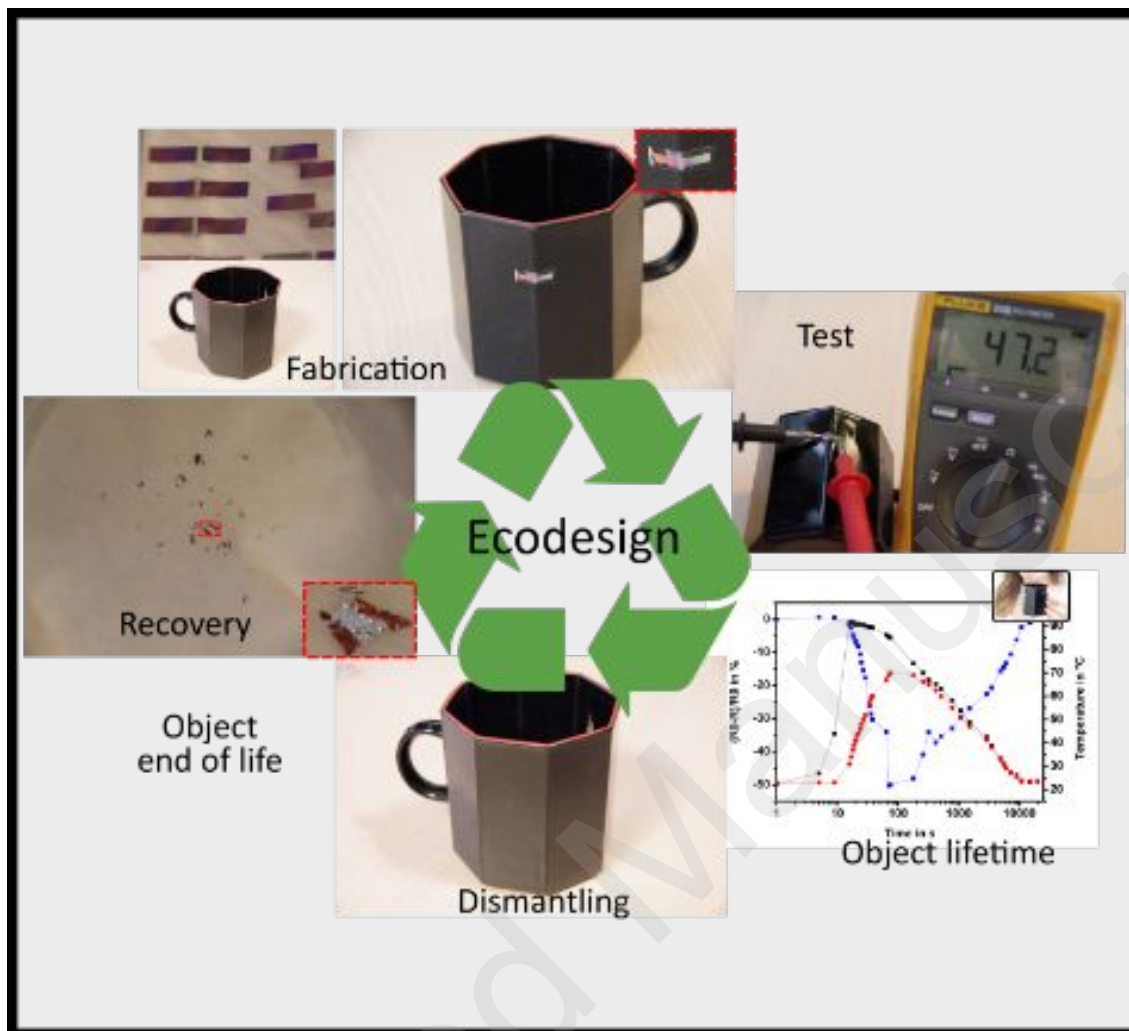
- 1
2
3
4 (10) Peng, X.; Yuan, J.; Shen, S.; Gao, M.; Chesman, A. S.; Yin, H.; Cheng, J.; Zhang,
5 Q.; Angmo, D. Perovskite and Organic Solar Cells Fabricated by Inkjet Printing:
6 Progress and Prospects. *Adv. Funct. Mater.* **2017**, *27*(41), 1703704.
7
8 (11) Adams, J. J.; Duoss, E. B.; Malkowski, T. F.; Motala, M. J.; Ahn, B. Y.; Nuzzo, R.
9 G.; Bernhard, J. T.; Lewis, J. A. Conformal Printing of Electrically Small Antennas
10 on Three-Dimensional Surfaces. *Adv. Mater.* **2011**, *23*(11), 1335–1340.
11
12 (12) Kraus, J. D.; Marhefka, R. J. Antennas for All Applications. *Antennas Appl. Kraus*
13 *John Daniel Marhefka Ronald J N. Y. McGraw-Hill C2002* **2002**.
14
15 (13) Salvatore, G. A.; Münzenrieder, N.; Kinkeldei, T.; Petti, L.; Zysset, C.; Strebel, I.;
16 Büthe, L.; Tröster, G. Wafer-Scale Design of Lightweight and Transparent
17 Electronics That Wraps around Hairs. *Nat. Commun.* **2014**, *5*, 2982.
18
19 (14) Rogers, J. A.; Someya, T.; Huang, Y. Materials and Mechanics for Stretchable
20 Electronics. *Science* **2010**, *327*(5973), 1603–1607.
21
22 (15) Zhang, Y.; Xu, S.; Fu, H.; Lee, J.; Su, J.; Hwang, K.-C.; Rogers, J. A.; Huang, Y.
23 Buckling in Serpentine Microstructures and Applications in Elastomer-Supported
24 Ultra-Stretchable Electronics with High Areal Coverage. *Soft Matter* **2013**, *9*(33),
25 8062.
26
27 (16) Kim, D.-H.; Lu, N.; Ma, R.; Kim, Y.-S.; Kim, R.-H.; Wang, S.; Wu, J.; Won, S. M.;
28 Tao, H.; Islam, A.; Yu, K. J.; Kim, T.-I.; Chowdhury, R.; Ying, M.; Xu, L.; Li M.; Chung,
29 H. J.; Keum, H.; McCormick, M.; Liu, P.; Zhang, Y-W; Omenetto, F. G.; Huan, Y.;
30 Coleman, T.; Rogers, J. A. Epidermal Electronics. *science* **2011**, *333*(6044), 838–
31 843.
32
33 (17) Rogel, R.; Borgne, B. L.; Mohammed-Brahim, T.; Jacques, E.; Harnois, M.
34 Spontaneous Buckling of Multiaxially Flexible and Stretchable Interconnects Using
35 PDMS/Fibrous Composite Substrates. *Adv. Mater. Interfaces* **2017**, *4*(3), 1600946.
36
37 (18) Yang, Y.; Vervust, T.; Dunphy, S.; Van Put, S.; Vandecasteele, B.; Dhaenens, K.;
38 Degrendele, L.; Mader, L.; De Vriese, L.; Martens, T.; Kaufmann, M.; Sekitani, T.;
39 Vanfleteren, J.. 3D Multifunctional Composites Based on Large-Area Stretchable
40 Circuit with Thermoforming Technology. *Adv. Electron. Mater.* **2018**, 1800071.
41
42 (19) Irimia-Vladu, M. “Green” Electronics: Biodegradable and Biocompatible Materials
43 and Devices for Sustainable Future. *Chem. Soc. Rev.* **2014**, *43*(2), 588–610.
44
45
46
47
48
49
50
51
52
53
54
55
56
57
58
59
60

- 1
2
3
4 (20) Irimia-Vladu, M.; Glowacki, E. D.; Voss, G.; Bauer, S.; Sariciftci, N. S. Green and
5 Biodegradable Electronics. *Mater. Today* **2012**, *15*(7–8), 340–346.
- 6
7 (21) Le Borgne, B.; Chung, B.-Y.; Tas, M. O.; King, S. G.; Harnois, M.; Sporea, R. A.
8 Eco-Friendly Materials for Daily-Life Inexpensive Printed Passive Devices: Towards
9 “Do-It-Yourself” Electronics. *Electronics* **2019**, *8*(6), 699.
- 10
11 (22) Moorthy, B.; Baek, C.; Wang, J. E.; Jeong, C. K.; Moon, S.; Park, K.-I.; Kim, D. K.
12 Piezoelectric Energy Harvesting from a PMN–PT Single Nanowire. *RSC Adv.* **2017**,
13 *7*(1), 260–265.
- 14
15 (23) Zhang, Y.; Sun, H.; Jeong, C. K. Biomimetic Porifera Skeletal Structure of Lead-
16 Free Piezocomposite Energy Harvesters. *ACS Appl. Mater. Interfaces* **2018**, *10*
17 (41), 35539–35546.
- 18
19 (24) Li, R.; Wang, L.; Kong, D.; Yin, L. Recent Progress on Biodegradable Materials and
20 Transient Electronics. *Bioact. Mater.* **2018**, *3*(3), 322–333.
- 21
22 (25) Fodil, K.; Denoual, M.; Dolabdjian, C.; Harnois, M.; Senez, V. Dynamic Sensing of
23 Magnetic Nanoparticles in Microchannel Using GMI Technology. *IEEE Trans.*
24 *Magn.* **2012**, *49*(1), 93–96.
- 25
26 (26) Yang, S.; Lu, N. Gauge Factor and Stretchability of Silicon-on-Polymer Strain
27 Gauges. *Sensors* **2013**, *13*(7), 8577–8594.
- 28
29 (27) French, P.; Evans, A. Piezoresistance in Polysilicon and Its Applications to Strain
30 Gauges. *Solid-State Electron.* **1989**, *32*(1), 1–10.
- 31
32 (28) Gleskova, H.; Wagner, S.; Soboyejo, W.; Suo, Z. Electrical Response of
33 Amorphous Silicon Thin-Film Transistors under Mechanical Strain. *J. Appl. Phys.*
34 **2002**, *92*(10), 6224–6229.
- 35
36 (29) Kervran, Y.; De Sagazan, O.; Crand, S.; Coulon, N.; Mohammed-Brahim, T.; Brel,
37 O. Microcrystalline Silicon: Strain Gauge and Sensor Arrays on Flexible Substrate
38 for the Measurement of High Deformations. *Sens. Actuators Phys.* **2015**, *236*, 273–
39 280.
- 40
41 (30) Faurie, D.; Renault, P.-O.; Le Bourhis, E.; Villain, P.; Goudeau, P.; Badawi, F.
42 Measurement of Thin Film Elastic Constants by X-Ray Diffraction. *Thin Solid Films*
43 **2004**, *469*, 201–205.
- 44
45
46
47
48
49
50
51
52
53
54
55
56
57
58
59
60

- 1
2
3
4 (31) Kaltenbrunner, M.; Sekitani, T.; Reeder, J.; Yokota, T.; Kuribara, K.; Tokuhara, T.;
5 Drack, M.; Schwödiauer, R.; Graz, I.; Bauer-Gogonea, S.; Bauer, S.; Someya, T.
6 An Ultra-Lightweight Design for Imperceptible Plastic Electronics. *Nature* **2013**, *499*
7 (7459), 458–463.
8
9
10 (32) Chortos, A.; Liu, J.; Bao, Z. Pursuing Prosthetic Electronic Skin. *Nat. Mater.* **2016**,
11 *15*(9), 937.
12
13 (33) Yang, S.; Chen, Y.-C.; Nicolini, L.; Pasupathy, P.; Sacks, J.; Su, B.; Yang, R.;
14 Sanchez, D.; Chang, Y.-F.; Wang, P.; Schnyer, D.; Neikirk, D.; Lu, N. “Cut-and-
15 Paste” Manufacture of Multiparametric Epidermal Sensor Systems. *Adv. Mater.*
16 **2015**, *27*(41), 6423–6430.
17
18 (34) Martinho, G.; Pires, A.; Saraiva, L.; Ribeiro, R. Composition of Plastics from Waste
19 Electrical and Electronic Equipment (WEEE) by Direct Sampling. *Waste Manag.*
20 **2012**, *32*(6), 1213–1217.
21
22 (35) Wang, Y.; Qiu, Y.; Ameri, S. K.; Jang, H.; Dai, Z.; Huang, Y.; Lu, N. Low-Cost, Mm-
23 Thick, Tape-Free Electronic Tattoo Sensors with Minimized Motion and Sweat
24 Artifacts. *Npj Flex. Electron.* **2018**, *2*(1), 6.
25
26 (36) Kabiri Ameri, S.; Ho, R.; Jang, H.; Tao, L.; Wang, Y.; Wang, L.; Schnyer, D. M.;
27 Akinwande, D.; Lu, N. Graphene Electronic Tattoo Sensors. *ACS Nano* **2017**, *11*
28 (8), 7634–7641.
29
30 (37) Kim, D.-H.; Viventi, J.; Amsden, J. J.; Xiao, J.; Vigeland, L.; Kim, Y.-S.; Blanco, J.
31 A.; Panilaitis, B.; Frechette, E. S.; Contreras, D.; Kaplan, D. L.; Omenetto F. G.;
32 Huang Y.; Hwang, K. C.; Zakin, M. R.; Litt, B.; Rogers, J. A. Dissolvable Films of
33 Silk Fibroin for Ultrathin Conformal Bio-Integrated Electronics. *Nat. Mater.* **2010**, *9*
34 (6), 511–517.
35
36 (38) Le Borgne, B.; Jacques, E.; Harnois, M. The Use of a Water Soluble Flexible
37 Substrate to Embed Electronics in Additively Manufactured Objects: From Tattoo to
38 Water Transfer Printed Electronics. *Micromachines* **2018**, *9*(9), 474.
39
40 (39) Ng, L. W.; Zhu, X.; Hu, G.; Macadam, N.; Um, D.; Wu, T.-C.; Moal, F. L.; Jones, C.
41 G.; Hasan, T. Conformal Printing of Graphene for Single and Multi-Layered Devices
42 on to Arbitrarily Shaped 3D Surfaces. *ArXiv Prepr. ArXiv181101073* **2018**.
43
44
45
46
47
48
49
50
51
52
53
54
55
56
57
58
59
60

- 1
2
3
4 (40) Saada, G.; Layani, M.; Chernevousky, A.; Magdassi, S. Hydroprinting Conductive
5 Patterns onto 3D Structures. *Adv. Mater. Technol.* **2017**, *2* (5), 1600289.
6
7 (41) Le Borgne, B.; Liu, S.; Morvan, X.; Crand, S.; Sporea, R. A.; Lu, N.; Harnois, M.
8 Water Transfer Printing Enhanced by Water-Induced Pattern Expansion: Toward
9 Large-Area 3D Electronics. *Adv. Mater. Technol.* **2019**, 1800600.
10
11 (42) Tao, H.; Brenckle, M. A.; Yang, M.; Zhang, J.; Liu, M.; Siebert, S. M.; Averitt, R. D.;
12 Mannoor, M. S.; McAlpine, M. C.; Rogers, J. A.; Kaplan, D. A.; Omenetto, F. G.
13 Silk-Based Conformal, Adhesive, Edible Food Sensors. *Adv. Mater.* **2012**, *24* (8),
14 1067–1072.
15
16 (43) Hwang, S.-W.; Park, G.; Edwards, C.; Corbin, E. A.; Kang, S.-K.; Cheng, H.; Song,
17 J.-K.; Kim, J.-H.; Yu, S.; Ng, J.; Lee, J. E.; Kim, J.; Yee, C.; Bhaduri, B.; Su, Y.;
18 Omenetto, F.G.; Huang, Y.; Bashir, R.; Goddard, L.; Popescu, G.; Lee, K.M.;
19 Rogers, J. A. Dissolution Chemistry and Biocompatibility of Single-Crystalline
20 Silicon Nanomembranes and Associated Materials for Transient Electronics. *ACS*
21 *Nano* **2014**, *8* (6), 5843–5851.
22
23 (44) Kang, S.-K.; Hwang, S.-W.; Cheng, H.; Yu, S.; Kim, B. H.; Kim, J.-H.; Huang, Y.;
24 Rogers, J. A. Dissolution Behaviors and Applications of Silicon Oxides and Nitrides
25 in Transient Electronics. *Adv. Funct. Mater.* **2014**, *24* (28), 4427–4434.
26
27
28
29
30
31
32
33
34
35
36
37
38
39
40
41
42
43
44
45
46
47
48
49
50
51
52
53
54
55
56
57
58
59
60

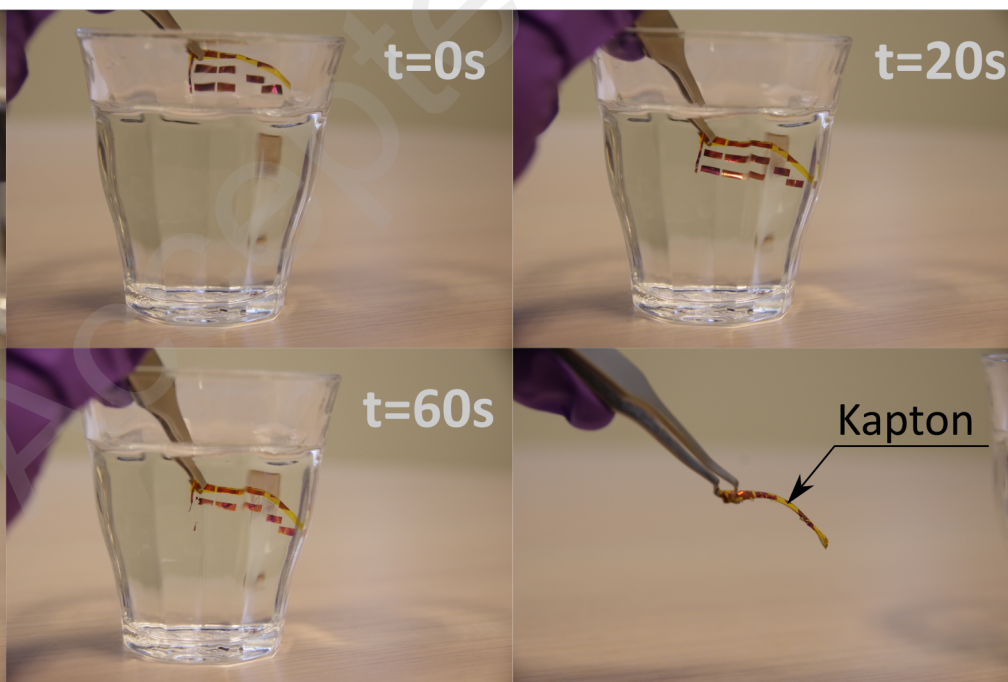
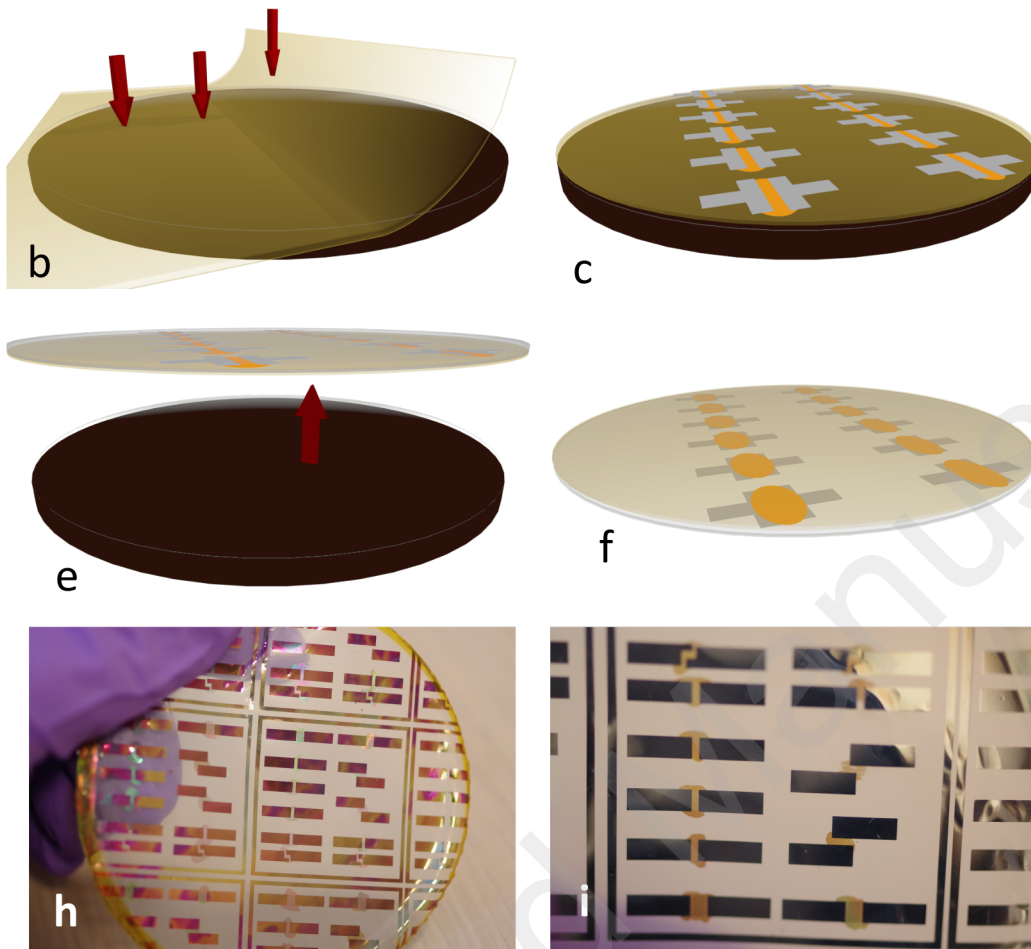
ToC figure

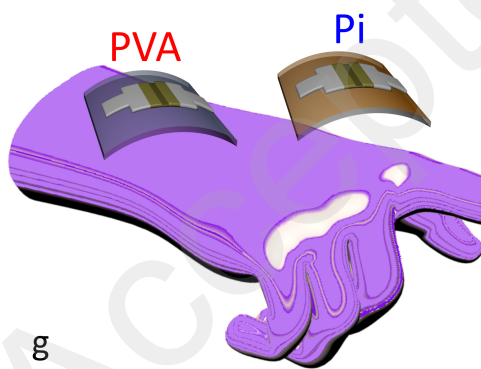
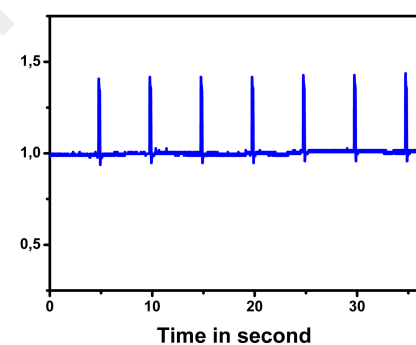
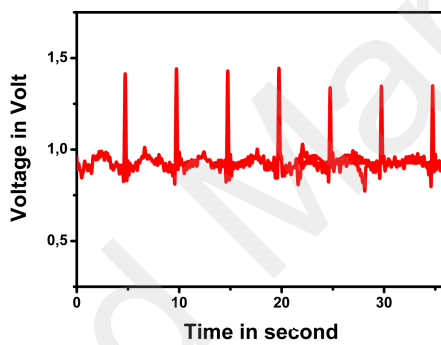
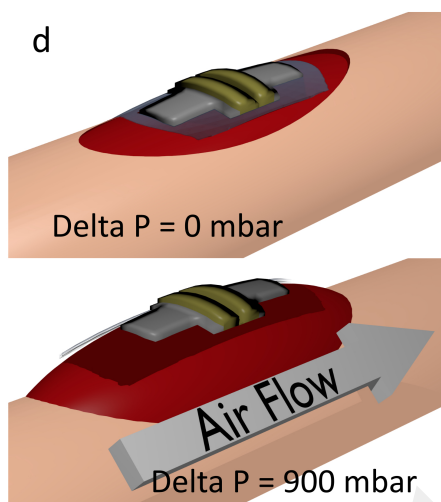
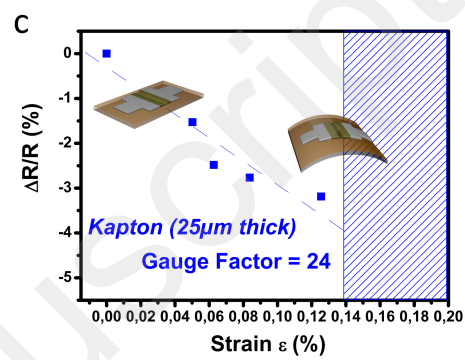
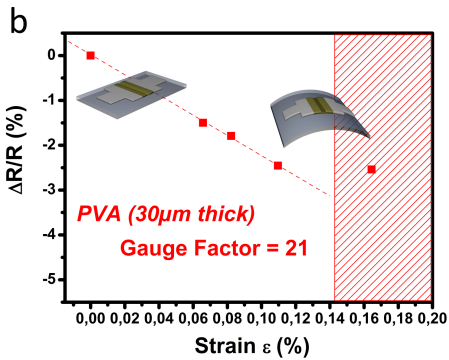
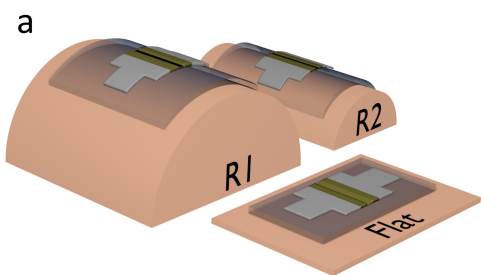


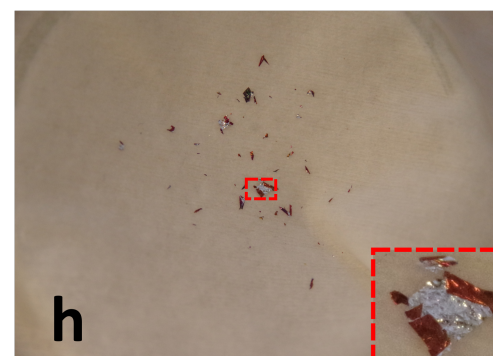
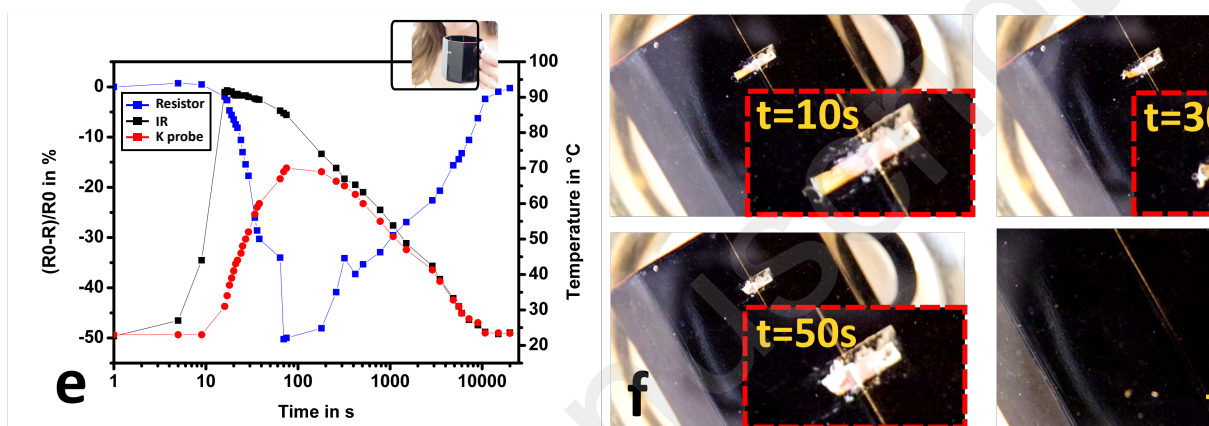
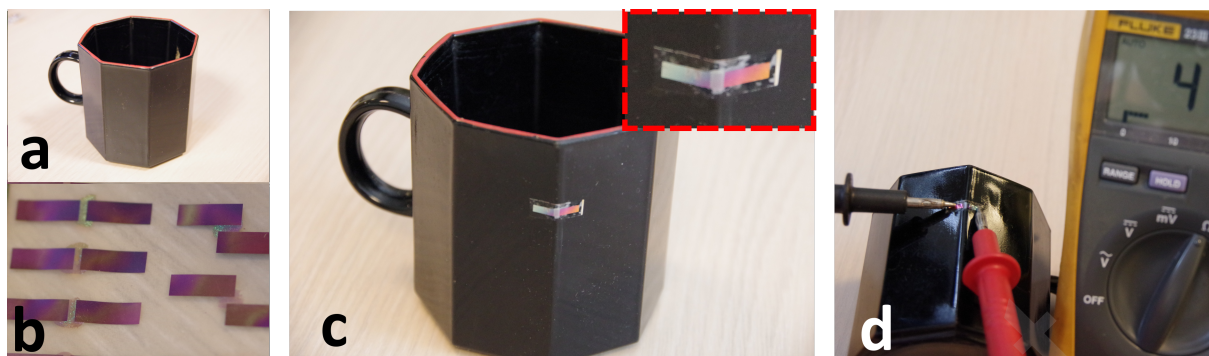
1
2
3
4
5
6
7
8
9
10
11
12
13
14
15
16
17
18
19
20
21
22
23
24
25
26
27
28
29
30
31
32
33
34
35
36
37
38
39
40
41
42
43
44
45
46
47
48
49
50
51
52
53
54
55
56
57
58
59
60

Accepted Manuscript

1
2
3
4
5
6
7
8
9
10
11
12
13
14
15
16
17
18
19
20
21
22
23
24
25
26
27
28
29
30
31
32
33
34
35
36
37
38
39
40
41
42
43
44
45
46
47
48
49
50
51
52
53
54
55
56
57
58
59
60







1
2
3
4
5
6
7
8
9
10
11
12
13
14
15
16
17
18
19
20
21
22
23
24
25
26
27
28
29
30
31
32
33
34
35
36
37
38
39
40
41
42
43
44
45
46
47
48
49
50
51
52
53
54
55
56
57
58
59
60

